THE JOURNAL OF PHYSICAL CHEMISTRY A
A JOURNAL OF THE AMERICAN CHEMICAL SOCIETY

pubs.acs.org/JPCA Article

Triple-T Method for Modeling Plasma-Assisted Ignition with Rich Vibrationally Excited States

Yifan Qiu, Yifei Zhu,* Zexing Qu,* and Yun Wu

Cite This: https://doi.org/10.1021/acs.jpca.5c03848 Read Online

ACCESS | Metrics & More | Article Recommendations

ABSTRACT: Vibrationally excited species play an important role in elevating the gas temperature and reaction rates in fuel−plasma reaction systems. Classical two-temperature models coupled with the well-known Fridman−Macheret α-model have been validated and widely used to describe the plasma and fuel systems. However, the Fridman−Macheret α-model strictly requires the information on elementary reaction rates. This, in conjunction with two-temperature models, may lead to high errors and high computational cost in high-dimensional plasma-combustion coupled modeling due to the enormous vibrationally related reactions and the misuse of overall rates in classical combustion chemistry sets. We propose in this work a three-temperature model (Triple-T model hereafter) as an option for modeling complex plasma-fuel chemistry systems. A new variation, "Reaction Temperature" T_{react}, is introduced to account for the influence of vibrationally excited states in high-dimensional models. This model has been successfully tested in 3 classical cases: the plasma-assisted ignition of $NH_3/O_2/N_2$, $CH_4/O_2/He$, and $H_2/O_2/He$ mixtures. The original chemistry set is reduced by 46%, 33%, and 7%, respectively. The influence of vibrational states on the energy partition and ignition delay time is studied with the help of the proposed model.

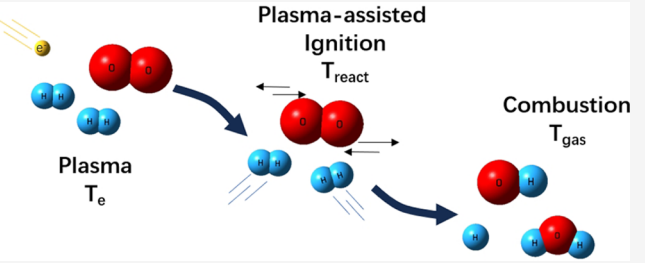

INTRODUCTION

Plasma-assisted ignition and energy conversion have attracted more and more attention in recent years. Plasma mainly promotes ignition through three pathways: the thermal effect via increasing gas temperature; the kinetic effect via producing excited state species and radicals; and the transport enhancement via fuel decomposition and ionic wind.[1,2]

About the thermal effect and kinetic effect of electronically and vibrationally excited species, there has been a lot of research: Mao et al. found that the long lifetime $O_2(a^1\Delta_g)$ produced in hybrid discharges is more efficient than O and $O(^1D)$ in ignition promotion with a given energy input.[3] The simulation study from Zhong et al. shows that the dissociation of NH_3 to NH/NH_2 at room temperature is controlled by electron collision and dissociative quenching by electronically excited species such as $N_2(A)$ and $O(^1D)$.[4] Taneja et al. found that the pressure-dependent recombination reaction $H + O_2 + M \rightarrow HO_2 + M$ can delay the ignition by limiting the reactive radicals.[5] The enhancement effects described above are all studied via global model coupling plasma chemistry and combustion chemistry.

The global modeling of coupled plasma and combustion chemistry primarily involves the coupling of the calculations from various programs. For example, Lefkowitz et al.[6] combined ZDPlaskin[7] with SENKIN[8] to establish the hybrid code coupling plasma and combustion chemistry. Based on the coupling of Cantera[9] and ZDPlaskin, Shahsavari et al.[10] developed a reaction kinetics model for the chemical coupling between plasma and combustion. We also developed a coupled plasma and combustion chemistry solver (named CPCC) by combining the ZDPlaskin code with a home-made simple combustion code with F90 format, adding a sensitivity and path flux analysis module to make the code compatible with widely used post-processing software (e.g., Pumpkin[11] and QtPlaskin[12]). During the discharge processes, ZDPlasKin utilizes a Boltzmann equation solver to determine the electron temperature and reaction rates, drawing from the input list of the electron impact reaction cross sections. SENKIN/Cantera is employed to compute the thermal properties and chemical reaction rates under conditions provided by ZDPlasKin. Additionally, integration of species and temperature equations is performed using an ODE solver, such as VODE.[13] These models have extensively examined the effects of electron collision reactions and chemical reactions involving electron excited states on the ignition. However, research into vibrationally excited states' impact on ignition remains insufficient.

Received: June 3, 2025
Revised: July 30, 2025
Accepted: July 31, 2025

The electron collision reaction generates a large number of vibrationally excited species, leading to a kinetic nonequilibrium process in the discharge.[14] In order to more accurately calculate the influence of the vibrationally excited state of plasma on the reaction, Gordiets et al.[15] used the "vibration temperature" to estimate the reaction rate constant. This estimation assumes that the vibrational levels conform to the Boltzmann distribution. Of course, when the vibrationally excited state distribution is far from the Boltzmann distribution, this estimation method may lead to certain inaccuracies. According to the Park model,[16] the dissociation rate coefficient can be determined using the conventional Arrhenius formula for equilibrium reactions, with temperature replaced by an effective value: $T_{\mathrm{eff}} = T_0^s T_v^{1-s}$. This implies the need to obtain the vibrational temperature, but real-time measurement of vibrational temperature in experiments requires strict experimental conditions.

In most plasma-assisted ignition studies, the Fridman−Macheret α-model is widely used to estimate the rate constants of chemical reactions in which vibrationally excited states participate, so that the contribution of vibrationally excited states to ignition is taken into account.[3,17,18] However, estimating reactions of all molecules in vibrationally excited states using solely the Fridman−Macheret α-model proves challenging: a large number of reaction rate estimates significantly increase the workload in constructing the reaction mechanism, making the model cumbersome and computationally demanding, particularly for two-dimensional (2D) and three-dimensional (3D) simulations. Meanwhile, a lack of comprehensive consideration for vibrationally excited states can potentially compromise the accuracy of simulation studies in plasma-assisted ignition.

The objective of this study is to develop a model that simplifies the consideration of vibrationally excited species in simulations of plasma-assisted ignition, reducing the number of reactions required while still ensuring computational accuracy. The Models and Chemistry Mechanisms section presents the development of a three-temperature model for plasma-assisted ignition, along with a corresponding mechanism establishment method. The verification of these components is conducted in the Performance of the Model and Chemistry Mechanisms section. The Effect of Vibrationally Excited Species in Different Discharge Conditions and Mixture section investigates the impact of vibrationally excited species on plasma-assisted ignition under varying initial temperature, pressure, and discharge conditions in $CH_4/O_2/He$ and $H_2/O_2/He$ mixtures, based on the newly developed model. The detailed calculation conditions are provided in the Discharge Definition and Initial Conditions section. Ultimately, the study concludes with a summary of findings in the Conclusions section.

MODELS AND CHEMISTRY MECHANISMS

Three-Temperature Model. Based on our previous coupled plasma and combustion chemistry solver (CPCC)[17] and the model from Ju et al.,[6] each time step is divided into two processes: the plasma chemistry process and the combustion chemistry process. By solving the following set of coupled rate equations, the time evolution of species density is obtained

$$\frac{\mathrm{d}[N_i]}{\mathrm{d}t} = \sum_{j=1}^{j_{\max}} S_{ij}(t) i = 1 \ldots i_{\max} \tag{1}$$

where $[N_i]$, S_{ij}, $i_{\max}$, and $j_{\max}$ represent the density of the i-th species, contribution of different reactions to the change in density of the i-th species, number of species, and reactions in the chemistry mechanisms, respectively. And the time evolution of gas temperature is obtained by calculating the energy change of the mixture

$$dH = c_{\mathrm{p}} \mathrm{d}T_{\mathrm{gas}} \tag{2}$$

$$dU = c_{v} \mathrm{d}T_{\mathrm{gas}} \tag{3}$$

where dT_{gas} is the change of gas temperature, dH and dU represent the enthalpy change and internal energy change of the mixture, respectively, and c_{p} and c_{v} represent the heat capacity at constant pressure and constant volume, respectively. Equation 2 is used in a constant-pressure environment, while eq 3 is applied in a constant-volume environment.

In the commonly used two-temperature global model, the discharge energy E_{ext} is divided into three parts: energy deposited into the electrons E_{elec}, the translational energy E_{gas}, and the chemical energy E_{chem}[19]

$$E_{\mathrm{ext}} = E_{\mathrm{gas}} + E_{\mathrm{elec}} + E_{\mathrm{chem}} \tag{4}$$

Energy used to calculate the change of gas temperature is E_{gas} (e.g., $E_{\mathrm{gas}} = dH$ in constant pressure calculation), which only includes the change in the translational energy. The vibrational energy is classified into the following categories: E_{chem}. The energy of the vibrationally excited species is transferred to E_{gas} through the inclusion of chemical and relaxation reactions involving vibrationally excited species in the chemistry mechanisms. This approach to separating energy and rate estimation leads to the following problems:

(i) Overly Complex Mechanism: Vibrationally excited states contribute to overcoming the energy barrier in almost all endothermic reactions. Thus, estimating all endothermic reactions using only the Fridman−Macheret α-model is challenging, and it leads to an excessively complex chemical mechanism, which makes it difficult to perform the computations within a reasonable time in 2D/3D simulations.

(ii) Unreasonable consideration of contributions from vibrational energy: The reaction rates in conventional combustion mechanisms generally include contributions from various vibrational energy levels. For instance, ref 20 computes the reaction rates for different vibrationally excited states and, using the Boltzmann distribution of these states, couples the rates from different vibrational levels into a single overall reaction rate. Furthermore, commonly used combustion reaction rates are typically validated or derived from shock tube experiments, which are unable to obtain reaction rates for a single vibrational energy level. However, as is shown in Figure 1, the "elementary reaction" required by the α-model specifically refers to the reaction rate involving the vibration level $v = 0$ only. Consequently, using classical combustion reaction rates in the α-model may overestimate the contribution of vibrational energy, especially when these rates are derived from global measurements, such as shock tube experiments. However, if well-characterized elementary rates are used (particularly those from high-level quantum calculations), the α-model can still yield reliable results, as shown in ref 18, though this significantly increases the workload required for mechanism development.

Inspired by the quasi-classical model described in ref 20, where contributions from different vibrational energy levels are incorporated into the reaction rate via the Boltzmann distribution, a similar approach is proposed for calculating reaction rates in nonequilibrium gases. By introducing a reduced temperature that simultaneously characterizes vibrational,

https://doi.org/10.1021/acs.jpca.5c03848
J. Phys. Chem. A XXXX, XXX, XXX−XXX

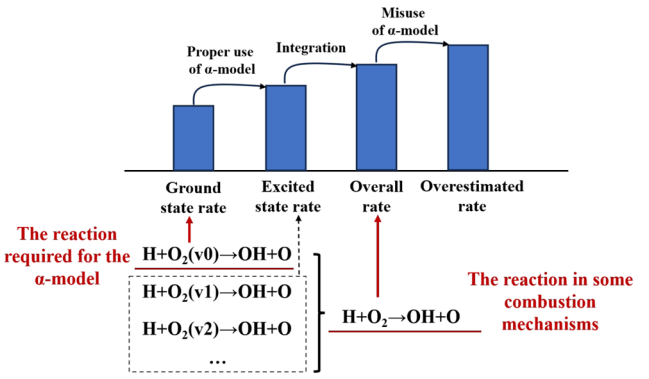

Figure 1. Schematic of the "ground-state reaction rate" required by the α-model and the "overall reaction rate" of the combustion mechanisms. Using combustion chemical mechanisms that include different vibrationally excited states for α-model estimation leads to an overestimation of the contribution of the vibrational energy to the reaction.

translational, and rotational energy modes, it is expected that the estimation of reaction rates can be significantly simplified, enabling more efficient and accurate computations (see Figure 2).

Therefore, our new model incorporates three distinct temperatures: the electron temperature T_{elec}, the experimentally measurable gas temperature T_{gas}, and the temperature T_{react} used to calculate the reaction rate constant. Unlike T_{gas}, T_{react} includes the energy of gas molecules' translational and vibrational energy rather than just involving the translational energy. The rotationally excited species are rapidly quenched due to the fast rotational−translational (R−T) relaxation,[14] thus the rotational energy is considered as translational energy.

T_{elec} is derived from the electron energy distribution function f_0[21]

$$T_{elec} = \int_0^\infty \varepsilon^{3/2} f_0 \, d\varepsilon \tag{5}$$

Here, ε symbolizes the electron energy. The computation of T_{elec} is performed by ZDPlaskin,[7] a plasma chemistry solver, in conjunction with the BOLSIG+[21] module, which is designed to solve the electron energy distribution function (EEDF). T_{elec} is utilized in the calculation of the rate constants for electron−related reactions, including electron−impact excitation and electron−impact dissociation, among others.

T_{gas} and T_{react} are calculated separately

$$\Delta T_{gas} = \frac{E_{gas}}{\bar{c}} \tag{6}$$

$$\Delta T_{react} = \frac{E_{react}}{\bar{c}} \tag{7}$$

$$E_{react} = E_{gas} + E_{vib} \tag{8}$$

Where $\bar{c}$, E_{react}, and E_{vib} represent the average heat capacity, the energy used to calculate the change of T_{react}, and the energy of the vibrationally excited state, respectively. E_{gas} can be calculated from eq 4. E_{vib} is determined by the change in the density of the vibrationally excited species over the iteration

$$E_{vib} = \sum_{i_{max}} E_{i,t+dt} \cdot n_{i,t+dt} - \sum_{i_{max}} E_{i,t} \cdot n_{i,t} \tag{9}$$

where $E_{i,t}$ and $n_{i,t}$ represent the energy and density of each vibrationally excited species in the mixture at time t, and $E_{i,t+dt}$ and $n_{i,t+dt}$ represent their energy and density at time $t + dt$. Different from T_{eff} in the existing Park model, T_{react}'s acquisition method is related to the energy change of the mixture and does not rely heavily on experimental measurement, so it has a wider applicability in simulation studies.

A pulse discharge under adiabatic conditions is used as an example to demonstrate the model (Figure 3). The process is divided into four stages based on different gas states: initial state, discharge stage, relaxation stage, and final equilibrium stage.

In the initial state (stage I), the gas is in equilibrium, with T_{gas} equal to T_{react}. In the discharge stage (Stage II), T_{react} rises rapidly due to the input of energy from the electric field. Rapid gas heating caused by the relaxation of electronically excited species also leads to a sharp increase in the T_{gas}. In low E/N conditions (as shown in Figure 3), a significant portion of the input energy is stored in vibrational modes, resulting in $T_{react} > T_{gas}$. In the relaxation stage (stage III), with no external energy input or loss, T_{react} remains constant, while vibrational energy gradually transfers to translational modes via V−T relaxation, slowly increasing T_{gas}. Eventually, in the final equilibrium stage (stage IV), the system returns to thermal equilibrium, with T_{gas} equaling T_{react} again.

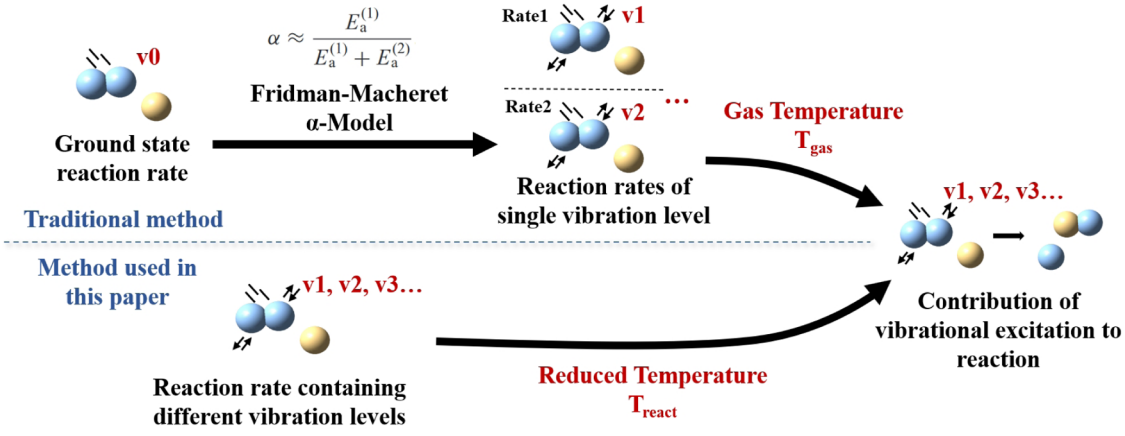

Figure 2. Diagram of a reaction rate based on a reduced temperature, as an alternative to the α-model. The α-model considers the contribution of vibration excitation to the reaction by estimating the reaction rate of a single vibration level. Based on the reduced temperature, the contribution of vibrational excitation to the reaction can be considered directly from the reaction rate containing different vibration levels.

https://doi.org/10.1021/acs.jpca.5c03848
J. Phys. Chem. A XXXX, XXX, XXX−XXX

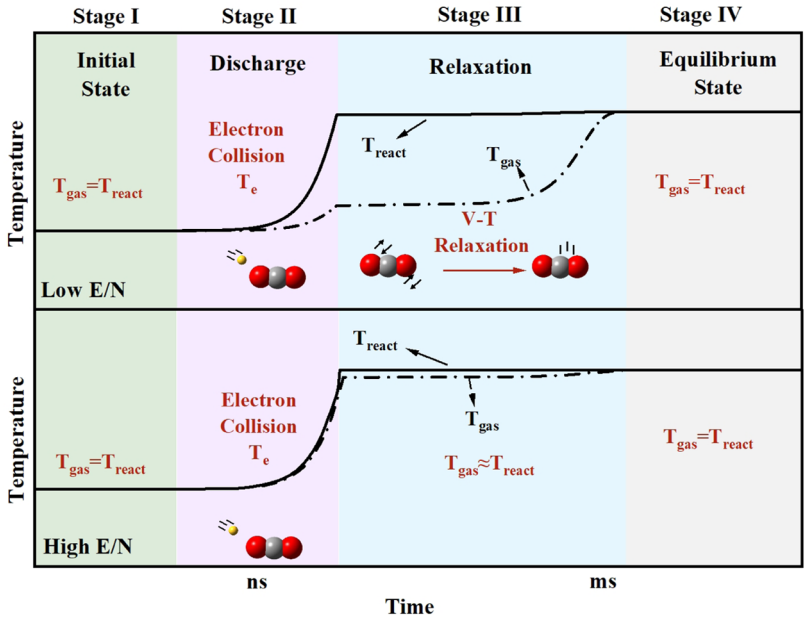

Figure 3. Diagram illustrating the differences and relationships between T_{gas} and T_{react} in the new model under adiabatic pulse discharge conditions.

Under high E/N conditions, however, the behavior in Stages II and III differs significantly. In this case, most of the input energy is consumed in electronic excitation, dissociation, and ionization, with little energy deposited in vibrational modes. As a result, the difference between T_{react} and T_{gas} is much smaller, and the two temperatures remain approximately equal ($T_{react} \approx T_{gas}$) throughout the discharge and relaxation stages.

Chemistry Mechanisms. The chemistry mechanisms consist of two components: combustion chemistry and plasma chemistry. The plasma chemistry mechanism includes chemical reactions and relaxation reactions involving vibrationally excited species. In the traditional global model, the reaction rate constants of chemical reactions involving vibrationally excited states are estimated using the Fridman−Macheret α-model.[16] In the Fridman-Macheret α-model, the rate constant of the ground-state species is used to estimate the reaction rate of the vibrationally excited state. The rate constants of ground-state species are mainly derived from traditional combustion chemistry mechanisms. Additionally, the rate constants of vibration−translation (V−T) relaxation and vibration−vibration (V−V) interactions are estimated using the SSH theory[16] and the Morse model,[22] respectively.

In this study, three groups of mechanisms were used: the $CH_4/O_2/He$ mechanism proposed by Mao et al.,[3] the $NH_3/O_2/N_2$ mechanism by Qiu et al.[17] and the $H_2/O_2/He$ mechanism also proposed by Mao et al.[18] These mechanisms include a comprehensive and detailed description of reactions involving vibrationally excited states.

The reactive enhancement of the vibrationally excited state has been considered in T_{react}; therefore, all of the chemical reactions involving vibrationally excited species are removed. To study the transfer of vibrational energy to translational energy, V−T relaxations and V−V interactions were preserved as the primary response to energy level changes in the vibrational state. With the aforementioned modifications, the plasma chemistry mechanism was significantly simplified. The number of plasma chemistry reactions in the $CH_4/O_2/He$, $NH_3/O_2/N_2$, and $H_2/O_2/He$ mechanisms was reduced from 629 to 339, 613 to 408, and 647 to 603, respectively.

A significant decrease in the number of reactions can improve not only the speed of zero-dimensional calculation but also facilitate the simplification of two-dimensional calculation mechanisms: a smaller mechanism scale can reduce the time required for sensitivity analysis during mechanism simplification. Meanwhile, this simplification helps to reasonably account for the contribution of vibrationally excited states to ignition in 2D/3D simulations.

Objectives and Limits of the Model. The objective of this work is to optimize the existing zero-dimensional model that couples plasma and combustion chemistry mechanisms. The proposed model aims to more comprehensively account for the impact of vibrationally excited states of each species on plasma-assisted ignition and energy conversion, diminish the workload created by numerous estimated rate constants, and decrease the complexity of the reaction mechanism, which can help to reduce the time cost in 2D/3D simulations. This model is expected to enhance the consideration of vibrationally excited states in 2D and 3D plasma-assisted ignition and energy conversion simulations.

Although this method addresses the issues of heavy computational workload and strict requirements on elementary reactions in the estimation based on the α-model, there are still areas for improvement. In the assumption of the model, it is considered that 100% vibrational energy is used to overcome the activation energy barrier of the reaction process. However, in fact, the utilization rate of vibrational energy in the reaction is not always 100%: for the strong endothermic reaction where the activation energy is close to the enthalpy of the reaction, the efficiency of vibrational energy α is the highest (close to 100%); but for exothermic reactions without activation energy, the efficiency of vibrational energy α is the lowest (close to 0%).[16] This means that for reactions that are less exothermic and endothermic, the use of this model leads to an overestimation of the rate due to the small vibrational energy contribution.

To overcome the above limitations, the model can be slightly adjusted during the calculations to minimize errors. Specifically, different temperatures can be used depending on the reaction type: for exothermic reactions, the reaction rate is determined

https://doi.org/10.1021/acs.jpca.5c03848
J. Phys. Chem. A XXXX, XXX, XXX−XXX

using T_{gas}, while for endothermic reactions, T_{react} is used. Alternatively, E_{vib} can be multiplied by an average α coefficient to calculate T_{react} based on the overall efficiency of vibrational energy utilization for the reaction. To avoid the high computational cost of determining reaction-specific α values, reactions can be broadly classified into three categories (endothermic, exothermic, and thermoneutral) with representative correction factors assigned to each type. The determination of these type-based correction factors is currently being investigated in our ongoing work using quantum chemistry methods.

Additionally, simplification of the mechanism results in the omission of certain reaction steps. As a result, the model lacks the capability to provide reliable quantitative predictions of the contributions from specific vibrationally excited states. This is because the model assumes that all vibrational energy can be used to overcome activation barriers, which is not rigorous from a microscopic perspective. However, this assumption serves as a practical compromise in macroscale chemical kinetics modeling, where reaction rates are governed by average molecular energy rather than the detailed energy distribution among degrees of freedom. In this context, the proposed method provides a simplified but effective alternative to the α-model, offering more robust qualitative information for 2D/3D simulations. As the ignition behavior in such simulations is often more sensitive to qualitative trends than exact vibrational state kinetics, this approach is especially suitable for large-scale modeling. We have clarified this point in response to the reviewer's concern.

Discharge Definition and Initial Conditions. A nanosecond hybrid DC discharge was employed to investigate the impact of the vibrationally excited species. The electron density was maintained through pulsed discharges, while the promotion of vibrationally excited species was achieved through low reduced electric field (E/N) discharges. The reduced electric field of the pulse was set to 200 Td, while the E/N of the DC stage ranged from 0 to 20 Td, which is comparable to the E/N values observed in gliding arc discharges, one of the most widely studied plasma sources in plasma-assisted combustion and energy conversion. The discharge frequency is fixed at 30 kHz.

In order to investigate the role of vibrationally excited species under various conditions, different initial temperatures and pressures were employed. The initial temperatures were set to 300, 450, 600, and 900 K, while the initial pressures were set to 250, 500, and 760 Torr. The mixture ratios for the different systems were as follows: 0.083 CH_4/0.167 O_2/0.75 He, 0.219 NH_3/0.164 O_2/0.617 N_2, and 0.1667 H_2/0.0833 O_2/0.75 He. All systems were considered adiabatic and maintained at a constant pressure.

RESULTS AND DISCUSSION

Performance of the Model and Chemistry Mechanisms. In this section, the performance of the model and the simplified chemical mechanism is examined.

To assess the model's ability to accurately capture the rapid gas heating resulting from the quenching of electronically excited states and the slow gas heating caused by the quenching of vibrationally excited states, we employed the model to simulate discharge in air and methane separately. The results are shown in Figure 4. In the air discharge, it can be seen that there are two obvious processes of fast gas heating and slow gas heating in T_{gas}, and the time evolution of T_{react} is also in line with expectations. Due to rapid V−T relaxation, the temperature difference in CH_4/O_2/He is extremely low, which is explained in

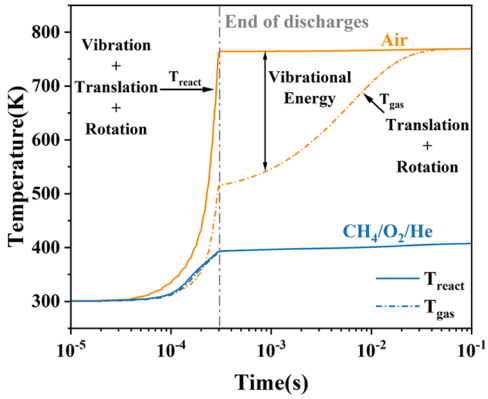

Figure 4. Evolution of T_{gas} and T_{react} over time during the discharge in air and a CH_4/O_2/He mixture. In air discharge, the difference between T_{gas} and T_{react} is significant, with T_{gas} showing two distinct increases. But in the CH_4 mixture, the difference between the two is negligible, and T_{gas} only exhibits a single increase.

The Effect of Vibrationally Excited Species in Different Discharge Conditions and Mixtures section. Overall, we believe that the model has the ability to simulate the transfer between different energies.

The simulated temperatures were compared with the experimental data from ref 6 and ref 4 to verify the new model and the reduced mechanism. Figure 5 shows that the simulation results are in good agreement with the experimental data for the low-temperature oxidation of 0.083 CH_4/0.167 O_2/0.75 He and 0.089 NH_3/0.084 O_2/0.827 N_2. Besides ensuring accuracy, the Triple-T model also significantly improves the calculation speed. As illustrated in Figure 5b, the calculation time for both CH_4/O_2/He and $NH_3/O_2/N_2$ mixtures is reduced by approximately 20%. This will provide a significant speed increase for both direct simulation and mechanism simplification of 2D/3D plasma-assisted combustion.

The comparison of experimental data for H_2/O_2/He mixtures in ref 18 is challenging due to the absence of energy loss data. Considering the excellent performance of the mechanism simplification method and the model in both CH_4/O_2/He and $NH_3/O_2/N_2$ mixtures, we believe that this method is also applicable to H_2/O_2/He mixtures.

Effect of Vibrationally Excited Species in Different Discharge Conditions and Mixtures. The effects of vibrationally excited species on ignition under different working conditions (initial temperature, pressure, and reduced field) and mixture are investigated in this section. Given the similar structure of CH_4 and NH_3 (involving the bonding of a heavy atom with hydrogen atoms), this section focuses on investigating the role of vibrationally excited species in CH_4/O_2/He and H_2/O_2/He mixtures.

Two parameters χ_{vib} and τ_{ign} are defined to study the proportion of vibrational excited species and their effect on the ignition delay. χ_{vib} and τ_{ign} are calculated using eqs 10 and 11, respectively

$$\chi_{vib} = \frac{T_{react} - T_{gas}}{T_{react}} \times 100\% \tag{10}$$

$$\tau_{ign} = \frac{\tau_{ign\text{-}2T} - \tau_{ign\text{-}3T}}{\tau_{ign\text{-}3T}} \times 100\% \tag{11}$$

https://doi.org/10.1021/acs.jpca.5c03848
J. Phys. Chem. A XXXX, XXX, XXX−XXX

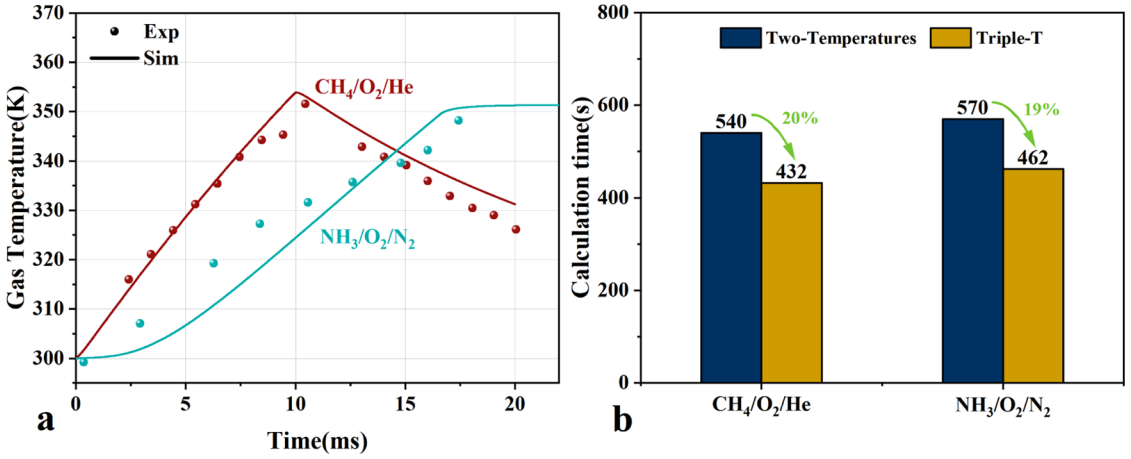

Figure 5. Comparison between (a) experimental and simulated results of gas temperature of plasma-assisted oxidation and (b) calculation time between the two-temperature model and Triple-T model in $CH_4/O_2/He$ and $NH_3/O_2/N_2$ mixtures.

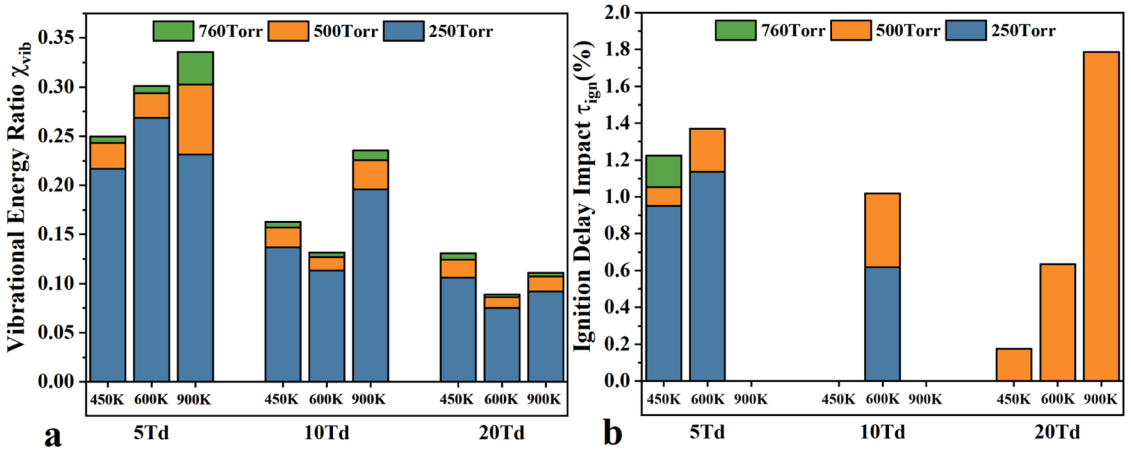

Figure 6. (a) Vibrational energy ratio χ_{vib} and (b) the ignition delay impact τ_{ign} for plasma-assisted 0.083 CH_4/0.167 O_2/0.75 He ignition with different E/N, temperatures, and pressures. χ_{vib} can quantify the proportion of vibrationally excited species in the mixture, and τ_{ign} indicates their effect on ignition.

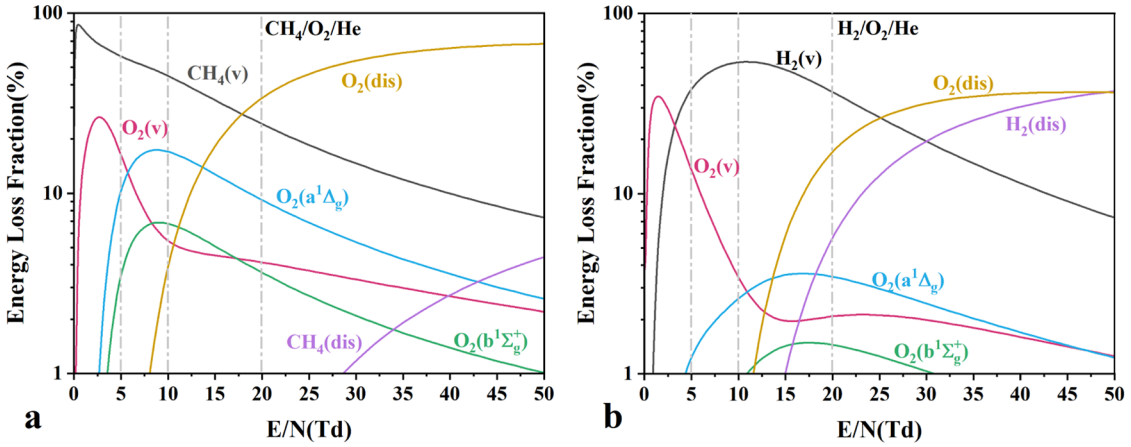

Figure 7. Energy loss fraction under different reduced electric fields in mixture (a) 0.083 CH_4/0.167 O_2/0.75 He and (b) 0.1667 H_2/0.0833 O_2/0.75 He.

where τ_{ign-2T} and τ_{ign-3T} represent the ignition delay time calculated using the three-temperature model and the traditional two-temperature model, respectively. χ_{vib} can be utilized to quantify the fraction of vibrationally excited species in the mixture, and τ_{ign} can show the influence of vibrationally excited species on ignition.

Figure 6 illustrates χ_{vib} and τ_{ign} during plasma-assisted ignition of a 0.083 CH_4/0.167 O_2/0.75 He mixture under various E/N of the DC stage, pressures, and initial temperatures. With an

https://doi.org/10.1021/acs.jpca.5c03848
J. Phys. Chem. A XXXX, XXX, XXX−XXX

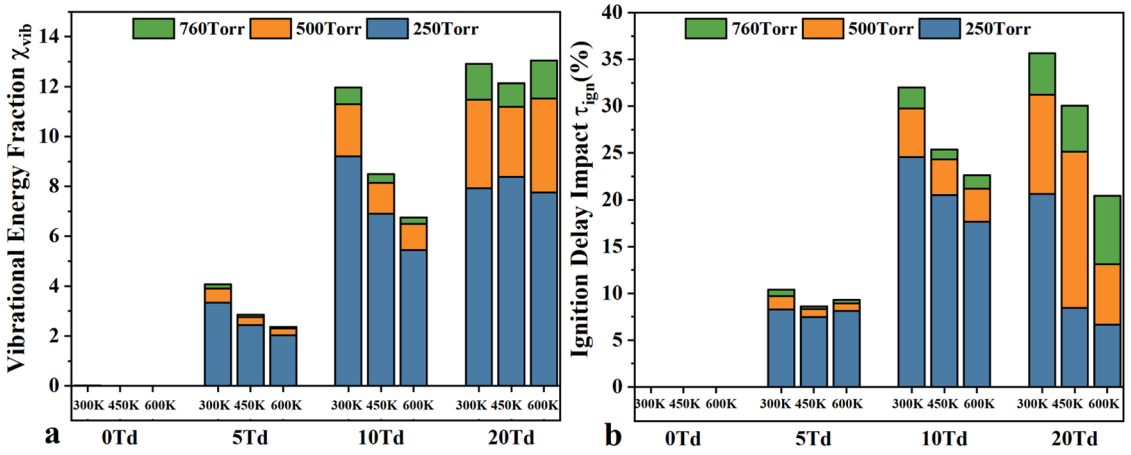

Figure 8. (a) Vibrational energy ratio χ_{vib} and (b) the ignition delay impact τ_{ign} for plasma−assisted 0.1667 H_2/0.0833 O_2/0.75 He ignition with different E/N, temperatures, and pressures. χ_{vib} can quantify the proportion of vibrationally excited species in the mixture, while τ_{ign} indicates their effect on the ignition.

increase in E/N from 5 to 20 Td, the energy deposited into CH_4(v) and O_2(v) decreases (see Figure 7a). Consequently, χ_{vib} in the CH_4/O_2/He mixture also decreases gradually (see Figure 6a). However, τ_{ign} does not exhibit a simple decrease with increasing E/N of the DC discharges. Specifically, τ_{ign} at 500 Torr shows a positive correlation with the reduced electric field: at 600 K, the E/N of the DC discharge increases from 5 to 20 Td, and τ_{ign} increases from about 0.25 to 0.75%. This phenomenon arises due to the decrease in the production of $O_2(a^1\Delta_g)$ when the E/N is approximately 10−20 Td. The reaction H + $O_2(a^1\Delta_g)$(+M) → HO_2(+M) exerts an inhibitory effect on ignition,[5,18] which becomes more pronounced at higher pressures. As the role of $O_2(a^1\Delta_g)$ in promoting ignition diminishes, the influence of vibrationally excited species on ignition becomes increasingly pronounced. Therefore, the change trend of the ignition delay time under 500 Torr differs from that under 250 Torr.

Overall, the impact of chemical reactions involving vibrationally excited species on ignition in CH_4/O_2/He mixtures is not significantly pronounced, with a maximum effect on the ignition delay time of only 2%. As a result, when establishing the chemistry mechanisms of hydrocarbon-based plasma-assisted combustion, it is unnecessary to devote excessive effort to considering the influence of vibrationally excited species on the ignition, as vibrational energy rapidly transfers to translational energy.

χ_{vib} and τ_{ign} of plasma-assisted 0.1667 H_2/0.0833 O_2/0.75 He ignition under different conditions are shown in Figure 8. Similar to the case of the CH_4/O_2/He mixture, in the case of pulse discharge (0 Td DC discharge), the energy deposition into vibrationally excited states is extremely low, resulting in a negligible influence on ignition. However, under 5−20 Td DC discharges, vibrational excitation has a significantly stronger effect in the H_2/O_2/He mixture than in CH_4/O_2/He: the H_2 mixture exhibits a χ_{vib} of up to 10% and a τ_{ign} of up to 25%, compared to only 1 and 2% in the CH_4/O_2 case.

This difference can be understood by comparing the characteristic time scales of key VT relaxation pathways, as listed in Table 1. The relaxation time of O_2(v1) by CH_4 is on the order of 10^{-8}−10^{-7} s, which is about 3 orders of magnitude faster than its relaxation by H_2 (typically 10^{-5} s). Consequently, the vibrational energy carried by O_2 is rapidly quenched in CH_4/O_2/He mixtures, limiting its contribution to ignition enhancement.

Table 1. Characteristic Times ($t = \ln(2)$/Rate, Unit: s) for VT Relaxation Reactions under Different Pressure and Temperature Conditions

conditions	O_2(v1) + H_2	O_2(v1) + N_2	O_2(v1) + CH_4
760 Torr, 300 K	1.52×10^{-5}	12.08	6.04×10^{-8}
250 Torr, 300 K	4.62×10^{-5}	36.73	1.84×10^{-7}
760 Torr, 600 K	1.81×10^{-6}	4.14×10^{-1}	1.68×10^{-8}
250 Torr, 600 K	5.51×10^{-6}	1.26	5.12×10^{-8}
conditions	H_2(v1) + H_2	H_2(v1) + O_2	CH_4(v1) + CH_4
760 Torr, 300 K	5.42×10^{-3}	3.39×10^{-2}	6.31×10^{-8}
250 Torr, 300 K	1.65×10^{-2}	1.03×10^{-1}	1.92×10^{-7}
760 Torr, 600 K	1.25×10^{-4}	7.79×10^{-4}	1.84×10^{-8}
250 Torr, 600 K	3.79×10^{-4}	2.37×10^{-3}	5.59×10^{-8}

In contrast, when O_2(v1) relaxes more slowly in H_2/O_2/He, vibrational energy is retained for a longer time, allowing more significant energy transfer to the thermal mode. Furthermore, direct excitation of H_2(v1), another primary vibrational energy channel in the H_2/O_2 mixture, also decays slowly: its VT relaxation by H_2 or O_2 is much slower (around 10^{-3}−10^{-2} s at 300 K, still above 10^{-4} s even at 600 K) compared to CH_4(v1) + CH_4, which is on the order of 10^{-8} s.

This again highlights that vibrational energy in the H_2/O_2 system persists over time scales relevant to ignition, while in CH_4/O_2, it is rapidly extinguished. Therefore, the observed stronger influence of vibrational excitation on ignition in H_2/O_2/He mixtures is a direct consequence of the slower vibrational relaxation of both O_2(v1) and H_2(v1), allowing for greater energy accumulation and coupling with the ignition process.

In addition, as shown in Figure 4, the relaxation time of the vibrationally excited state in pure air is longer than the typical time required for plasma-assisted ignition (10−100 μs). This implies that the reaction temperature of the gas will be higher than the measured temperature owing to the significant presence of vibrationally excited states during air gliding arc plasma-assisted combustion.

Another distinction from the CH_4/O_2/He mixture in Figure 8 is that the influence of the vibrationally excited species on the ignition delay time in the H_2/O_2/He mixture is essentially proportional to the average temperature difference. This is

https://doi.org/10.1021/acs.jpca.5c03848
J. Phys. Chem. A XXXX, XXX, XXX−XXX

because the energy used to produce the aforementioned equilibria $O_2(a^1\Delta_g)$ in the $H_2/O_2/He$ mixture is about 10% lower than that in the $CH_4/O_2/He$ mixture, resulting in a minimal impact of $O_2(a^1\Delta_g)$ on the ignition delay time. Consequently, the ignition delay in low E/N plasma-assisted $H_2/O_2/He$ ignition is primarily influenced by the vibrationally excited species.

The energy deposition of the vibrationally excited state reaches its peak at 10 Td and subsequently decreases. Therefore, in Figure 8b, within the range 0 to 10 Td, the influence of the vibrationally excited state on the ignition delay time gradually increases (from 0 to 15−25%), but this influence decreases at 10−20 Td (from 15−25 to 7−22%). Additionally, as the pressure increases from 250 to 760 Torr, the average temperature difference gradually diminishes from 8% to less than 2%. This occurs because the gas becomes thin at low pressure, resulting in a lower collision probability for V−T relaxation, but the reaction rate of the electron collision reaction is not so much affected by the pressure: the electron collision reaction rate is only linear with the gas density and not the square relationship of the V−T reaction. Thus, the reaction rate of V−T relaxation decreases faster than the electron collision reaction, which leads to the presence of more vibrationally excited species. Consequently, the influence of vibrationally excited states becomes more pronounced at low pressure.

CONCLUSIONS

A three-temperature model that hybrid plasma chemistry and combustion chemistry has been developed to enhance the simulation of the effects of vibrationally excited species on ignition. Meanwhile, a simplified method for establishing mechanisms has been formulated. This method eliminates the need for the Fridman−Macheret α-model to estimate the chemical reactions involved in the vibrationally excited state, focusing just on V−V and V−T relaxation, which can reduce the reactions of the plasma mechanism by about 30−40%, which also facilitates 2D/3D simulations. This approach considerably reduces the calculation time. The new model better reflects the microscopic interpretation of temperature as a result of translational, rotational, and vibrational molecular motion and accurately captures both the rapid and slow gas heating processes during air discharge. Additionally, the model can effectively reproduce the experimental data by using the simplified mechanism.

To study the role of vibrationally excited species in plasma-assisted combustion, pulsed hybrid DC discharges are used to approximate a gliding arc discharge, which features rich vibrationally excited species. The plasma-assisted ignition of the $CH_4/O_2/He$ mixture and the $H_2/O_2/He$ mixture is simulated. The results are as follows:

(i) In plasma-assisted ignition with low reduced electric field, the reactions containing vibrationally excited states in hydrocarbon fuel are almost negligible, but not in hydrogen. Because vibrational energy rapidly converts to translational energy, the impact of vibrationally excited state chemical reactions on the ignition delay time in hydrocarbon fuel is minimal, typically around 2% at most. Conversely, in plasma-assisted hydrogen combustion, the slow relaxation of vibrationally excited states results in a relatively high proportion of vibrationally excited energy (2−10%), leading to a more pronounced effect on the ignition delay time, reaching a maximum of 25%.

(ii) The impact of temperature, pressure, and E/N of DC discharges on vibrationally excited states in plasma-assisted combustion is substantial. In both $CH_4/O_2/He$ and $H_2/O_2/He$, the proportion of vibrational excited state energy diminishes as the pressure and temperature increase. Yet, the impact of vibrationally excited state energy on the E/N of DC discharges is not consistently monotonic, owing to the interaction between the energy deposited into the vibrationally excited state and $O_2(a^1\Delta_g)$. Moreover, the influence of the vibrationally excited state on ignition is not positively correlated. The ignition under pulse hybrid 5−20 Td E/N DC discharges results from the interaction between the vibrationally excited state and the $O_2(a^1\Delta_g)$.

The fundamental conclusion that the influence of vibrationally excited state reactions in hydrocarbon fuels is essentially negligible can offer theoretical support for developing and streamlining the chemical mechanism. In low E/N discharges or pulse discharges with a short rising edge, reducing the consideration of vibrationally excited species can significantly enhance the study efficiency. However, the model still exhibits some deficiencies, including specific errors related to the assumption of vibrational energy distribution as a Boltzmann distribution. More precise methods for expressing vibrational energy will be developed based on this model in the future.

AUTHOR INFORMATION

Corresponding Authors

Yifei Zhu − *National Key Lab of Aerospace Power System and Plasma Technology, Xi'an Jiaotong University, Xi'an 710049, China*; Email: yifei.zhu.plasma@gmail.com

Zexing Qu − *Institute of Theoretical Chemistry, College of Chemistry, Jilin University, Changchun 130023, China*; orcid.org/0000-0003-3445-4003; Email: zxqu@jlu.edu.cn

Authors

Yifan Qiu − *National Key Lab of Aerospace Power System and Plasma Technology, Xi'an Jiaotong University, Xi'an 710049, China*; orcid.org/0009-0003-9162-1610

Yun Wu − *National Key Lab of Aerospace Power System and Plasma Technology, Xi'an Jiaotong University, Xi'an 710049, China*

Complete contact information is available at: https://pubs.acs.org/10.1021/acs.jpca.5c03848

Notes

The authors declare no competing financial interest.

ACKNOWLEDGMENTS

The work is supported by the National Natural Science Foundation Basic Science Center Project (52488101), the National Key Research and Development Program of China (2022YFC2604002), and the National Natural Science Foundation of China (No.52277168, 52025064, 92271113). The authors thank the young research group in Atelier des Plasmas for fruitful discussions and the Gongfang Tech Co, Ltd for technical support.

REFERENCES

(1) Ju, Y.; Lefkowitz, J. K.; Reuter, C. B.; Won, S. H.; Yang, X.; Yang, S.; Sun, W.; Jiang, Z.; Chen, Q. Plasma assisted low temperature combustion. *Plasma Chem. Plasma Process.* **2016**, *36*, 85−105.

(2) Ju, Y.; Sun, W. Plasma assisted combustion: Dynamics and chemistry. *Prog. Energy Combust. Sci.* **2015**, *48*, 21−83.

(3) Mao, X.; Rousso, A.; Chen, Q.; Ju, Y. Numerical modeling of ignition enhancement of CH_4/O_2/He mixtures using a hybrid repetitive nanosecond and DC discharge. *Proc. Combust. Inst.* **2019**, *37*, 5545−5552.
(4) Zhong, H.; Mao, X.; Liu, N.; Wang, Z.; Ombrello, T.; Ju, Y. Understanding non-equilibrium N_2O/NOx chemistry in plasma-assisted low-temperature NH_3 oxidation. *Combust. Flame* **2023**, *256*, No. 112948.
(5) Taneja, T. S.; Johnson, P. N.; Yang, S. Nanosecond pulsed plasma assisted combustion of ammonia-air mixtures: Effects on ignition delays and NOx emission. *Combust. Flame* **2022**, *245*, No. 112327.
(6) Lefkowitz, J. K.; Guo, P.; Rousso, A.; Ju, Y. Species and temperature measurements of methane oxidation in a nanosecond repetitively pulsed discharge. *Philos. Trans. R. Soc., A* **2015**, *373*, No. 20140333.
(7) Pancheshnyi, S.; Eismann, B.; Hagelaar, G.; Pitchford, L. Computer code ZDPlasKin 2008 http://www.zdplaskin.laplace.univ-tlse.fr.
(8) Lutz, A. E.; Kee, R. J.; Miller, J. A. *SENKIN: A FORTRAN Program for Predicting Homogeneous Gas Phase Chemical Kinetics with Sensitivity Analysis*; U.S. Department of EnergyOffice of Scientific and Technical Information, 1988.
(9) Goodwin, D. G.; Moffat, H. K.; Speth, R. L. Cantera: An Object-Oriented Software Toolkit for Chemical Kinetics, Thermodynamics, and Transport Processes 2021. https://www.cantera.org.
(10) Shahsavari, M.; Konnov, A. A.; Valera-Medina, A.; Jangi, M. On nanosecond plasma-assisted ammonia combustion: Effects of pulse and mixture properties. *Combust. Flame* **2022**, *245*, No. 112368.
(11) Markosyan, A. H.; Luque, A.; Gordillo-Vázquez, F. J.; Ebert, U. PumpKin: A tool to find principal pathways in plasma chemical models. *Comput. Phys. Commun.* **2014**, *185*, 2697−2702.
(12) Pannier, E.; Ivko, S. QTPlaskin 2020. https://github.com/aluque/qtplaskin/.
(13) Brown, P. N.; Byrne, G. D.; Hindmarsh, A. C. VODE: A variable-coefficient ODE solver. *SIAM J. Sci. Stat. Comput.* **1989**, *10*, 1038−1051.
(14) Starikovskiy, A.; Aleksandrov, N. Plasma-assisted ignition and combustion. *Prog. Energy Combust. Sci.* **2013**, *39*, 61−110.
(15) Gordiets, B. F.; Ferreira, C. M.; Guerra, V. L.; Loureiro, J. M.; Nahorny, J.; Pagnon, D.; Touzeau, M.; Vialle, M. Kinetic model of a low-pressure N_2-O_2 flowing glow discharge. *IEEE Trans. Plasma Sci.* **1995**, *23*, 750−768.
(16) Fridman, A. *Plasma Chemistry*; Cambridge University Press, 2008.
(17) Qiu, Y.; Zhu, Y.; Wu, Y.; Zhao, N.; Li, Z.; Hao, M.; Zhang, B.; Pan, D. Numerical investigation of the hybrid pulse-DC plasma assisted ignition and NOx emission of $NH_3/N_2/O_2$ mixture. *Combust. Flame* **2023**, *258*, No. 113078.
(18) Mao, X.; Chen, Q.; Rousso, A. C.; Chen, T. Y.; Ju, Y. Effects of controlled non-equilibrium excitation on H_2/O_2/He ignition using a hybrid repetitive nanosecond and DC discharge. *Combust. Flame* **2019**, *206*, 522−535.
(19) Flitti, A.; Pancheshnyi, S. Gas heating in fast pulsed discharges in N_2-O_2 mixtures. *Eur. Phys. J. Appl. Phys.* **2009**, *45*, No. 21001.
(20) Peslherbe, G. H.; Wang, H.; Hase, W. L. Monte Carlo sampling for classical trajectory simulations. *Adv. Chem. Phys.* **1999**, *105*, 171−201.
(21) Hagelaar, G. J. M.; Pitchford, L. C. Solving the Boltzmann equation to obtain electron transport coefficients and rate coefficients for fluid models. *Plasma Sources Sci. Technol.* **2005**, *14*, No. 722.
(22) Capitelli, M.; Ferreira, C. M.; Gordiets, B. F.; Osipov, A. I. *Plasma Kinetics in Atmospheric Gases*; Springer Science & Business Media, 2013; Vol. *31*.

https://doi.org/10.1021/acs.jpca.5c03848
J. Phys. Chem. A XXXX, XXX, XXX−XXX